Buckling of Elastomeric Beams Enables Actuation of Soft Machines

*Dian Yang, Bobak Mosadegh, Alar Ainla, Benjamin Lee, Fatemeh Khashai, Zhigang Suo, Katia Bertoldi, and George M. Whitesides**

Historically, many machines (especially robots) were designed to mimic the motions of humans and other animals, but to add power, speed, "endurance," and reproducibility to those motions.[1] The robots on industrial assembly lines, for example, extend the capabilities of the workers that originally carried out assembly by hand using simple tools, by adding power, complex tools, indifference to environmental conditions, and mechanical "endurance." Similarly, four-wheeled robots are loosely derived from four-limbed animals, and aerial drones can be traced in design backward in time through manned aircraft, to birds. Conventional machines-especially those fabricated from metal, ceramics, and structural polymers (so-called "hard" machines)-can carry out almost arbitrarily complex motions using pulleys, cables, gears, and electric or hydraulic actuators. To achieve controlled motion, however, they also normally require complex systems for active controls (networks of sensors, actuators, and feedback controllers).[2,3] Some of these "hard" systems are exquisitely and highly developed, but can be heavy, energy inefficient, dangerous to humans, and expensive.

We are exploring soft actuators and robots-machines modeled after simpler animals (e.g., starfish, worms, and squid) having no hard internal or external structures, and fabricated entirely or predominantly in soft, compliant polymers.[4,5] The first generation of these systems-originally sketched by Suzumori et al.,[6–8] and then realized and elaborated by us,[5,9–13] and by others[4]-use pneumatic actuators, comprising networks of microchannels; in our systems, differential expansion of these pneumatic networks (PneuNets) by pressurization using air produces motions (especially bending, curling, and variants on them) that are already established as useful in grippers, and interesting for their potential in walkers, tentacles, and a number of other soft, actuated systems.[14] Although the design of the first of these systems has been relatively simple, the motion they produce on actuation can be surprisingly sophisticated: for example, a representative structure-the "finger" or "tentacle" of a gripper-curls nonuniformly, starting from its tip and proceeding to its stem, although the pressure applied in the PneuNet is approximately uniform throughout the system of inflatable channels.[10,11] This motion reflects a nonlinear property of soft materials and structures, referred to as a "snap-through instability."[15–19] Although nonlinear properties of materials are often considered a disadvantage, this type of nonlinearity, illustrated by snap-through, and other complex mechanical characteristics of soft systems, are proving to be useful, and to offer new capabilities to effectors, machines, and robots, because they enable a range of motions of sufficient complexity that-although they might be possible to replicate in a hard robotic system[20]-it would be complicated and expensive to do so.

This article demonstrates the utility of another type of nonlinear behavior-the reversible, cooperative torsion, and collapse of a set of elastomeric beams (fabricated as one connected piece) under pressure. Understanding the motions exhibited in these systems started with observations and analyses by Boyce and co-workers[21,22] of cooperative transformations in the shapes of patterns of through-holes cut into elastomeric slabs, on applying external pressure to these structures in the plane of the slab. Our work extends these studies, and greatly increases the ability of this kind of system, by using negative pressure (e.g., vacuum) applied to an elastomeric structure containing a number of elastic beams and interconnected, deformable cavities sealed within a thin elastomeric membrane. When negative pressure is applied, cooperative interactions among the components of the structure cause its elements (beams) to bend and buckle in ways that produce a range of useful motions.

Buckling of materials is ordinarily considered an undesired mode of mechanical and structural failure, as it causes permanent damage to structural components (e.g., metal frames, concrete pillars).[23,24] The buckling of elastomeric materials, however, is reversible, and can provide useful new functions when designed properly. One such useful function is a rotary motion that provides a torque.

The design of a typical structure (**Figure 1**), which we refer to as a "single-unit buckling actuator" or a "buckling actuator unit", consists of an elastomeric structure with a "nonbuckling center area" connecting to several (in most of our systems, four) "buckling pillars." This elastic framework, together with a thin (1 mm) top and bottom membrane, separates several cylindrical "deflation chambers" (in Figure 1, four). These chambers are all connected to a single inlet/outlet tube for pneumatic or fluidic actuation. The thinnest region of the buckling pillars is 2 mm in width, and the major and minor axes of the elliptical

D. Yang, Dr. B. Mosadegh, Dr. A. Ainla, B. Lee, F. Khashai, Prof. G. M. Whitesides
Department of Chemistry and Chemical Biology
Harvard University
12 Oxford Street, Cambridge, MA 02138, USA
E-mail: gwhitesides@gmwgroup.harvard.edu
D. Yang, Prof. Z. Suo, Prof. K. Bertoldi
School of Engineering and Applied Sciences Harvard University
29 Oxford Street, Cambridge, MA 02138, USA
Dr. B. Mosadegh, Prof. G. M. Whitesides
Wyss Institute for Biologically Inspired Engineering Harvard University
60 Oxford Street, Cambridge, MA 02138, USA
Prof. Z. Suo, Prof. K. Bertoldi, Prof. G. M. Whitesides
Kavli Institute for Bionano Science & Technology Harvard University
29 Oxford Street, Cambridge, MA 02138, USA

DOI: 10.1002/adma.201503188

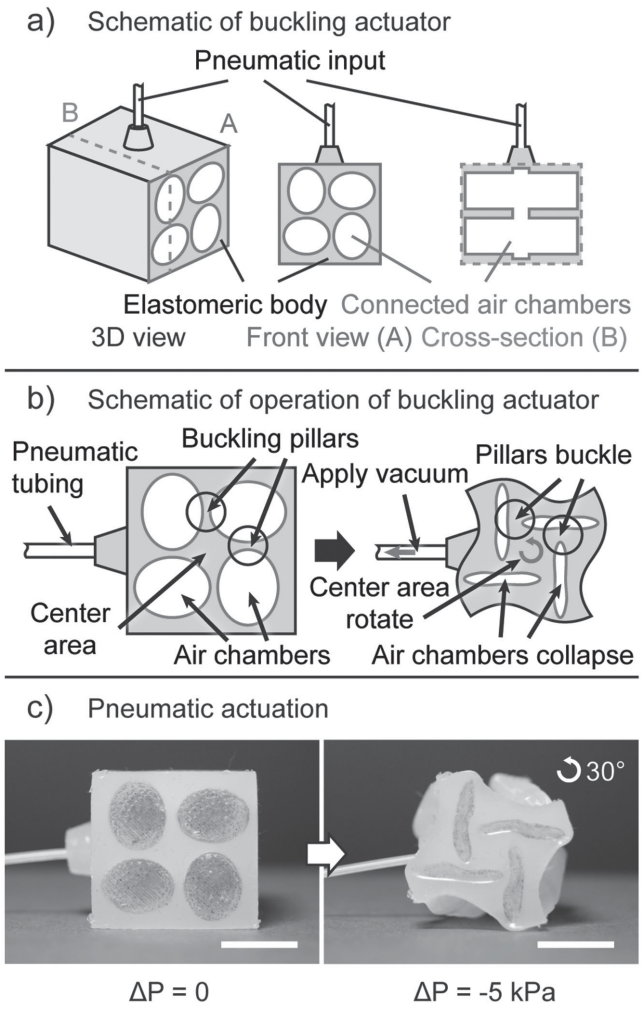

Figure 1. Schematics of a single-unit buckling actuator. a) A buckling actuator unit consists of an elastomeric structure with a nonbuckling center area connecting to several buckling pillars, with air chambers in between. The air chambers are actuated externally through a single pneumatic input. b) The rotary actuation mechanism of buckling actuator. Vacuum induces overall compression of the structure, causing the buckling pillars to deform into predetermined shapes. The cooperative deformation causes the center area to rotate in one preferred direction. c) Images of a single-unit buckling actuator in the initial and the fully actuated state. The inside of the chambers are colored with a black marker to visualize its boundary. Scale bars are 1 cm.

air chambers are 10 and 8 mm, respectively. The structure in Figure 1 has a square-shaped front surface, with dimensions 22 × 22 mm, and is 28 mm thick. We fabricated the entire structure in several pieces, using silicone elastomer cured in a mold fabricated from acrylonitrile butadiene styrene (ABS) and generated using a 3D printer (Figure S1, Supporting Information).

Applying vacuum induces an overall compression of the structure, as a reflection of the difference between the external (atmospheric) pressure, and the internal (10–100 kPa, 0.1–1 atm) pressure. This compression causes the pillars to buckle, and thus to deform into bent shapes. (Euler buckling[25] happens when pillars or beams are subject to compression.) The direction of bending is predetermined by a misalignment of the pillars relative to the center area, which in turn causes the center area to rotate in one preferred direction. For example, in our structure, the buckling pillars are all aligned in a way which causes a preferred counter-clockwise rotation (Figure 1b,c, Supporting video: single_actuation_unit.mp4). The relationship between the angle of rotation and pressure input is nonlinear (Figure S2, Supporting Information). This geometry yields a maximum angle of rotation of ≈30°.

We characterize and discuss proof-of-concept applications of this type of buckling actuator using the "fourfold symmetric design," in which four pillars are attached to the center area (Figure 1). Buckling actuators of other symmetries, which yield different magnitudes of rotation (from 10° to 30°) and torque, can be found in the Supporting Information (Figure S3, Supporting video: triangular_rotator.mp4, pentagonal_rotator.mp4, hexagonal_rotator.mp4).

We use pneumatic actuation in our design for obvious reasons: air is widely available, environmentally benign, lightweight, safe, easy to transfer (because of low viscosity); its flows can also be controlled and monitored using simple regulators, valves, and sensors.

Multiple buckling actuators units can be positioned in parallel and actuated with a connected/shared pneumatic input (**Figure 2**). A "multi-unit buckling actuator" consists of multiple "nonbuckling center areas" that each connects to several (in most of our systems, four) "buckling pillars." Figure 2a,b shows a buckling actuator with two actuation units, and Figure 2c shows a buckling actuator with a 3 × 4 array of actuation units (Supporting video: buckling_actuator_1×2.mp4, buckling_actuator_3×4.mp4).

Figure 2d demonstrates that buckling actuators can generate parallel motions. We attached 12 square tiles to the 12 rotating centers of a 3 × 4 buckling actuator. When vacuum (≈10 kPa differential pressure) is applied to the actuator, the tiles rotate synchronously but in different directions in a manner that brings them into alignment. When the internal pressure of the actuator is restored to ambient, the tiles rotate simultaneously back to their original positions (Supporting video: Big_H.mp4).

The buckling actuators can also be put in series (i.e., stacked). Stacking two buckling actuators that rotate in the same direction in series results in a larger rotation relative to one another (Figure 2e, the relative rotation angle is represented by the two flags, Supporting video: Rotation_chiral.mp4), and stacking two that rotate in different directions results in a zero net relative rotation (Figure 2f, Supporting video: Rotation_mirror.mp4).

Buckling actuators of different rotational symmetry can also be parallelized. The Supporting Information (Figure S4, Supporting video: triangular_rotator_6.mp4, hexagonal_rotator_3.mp4) shows two generic examples (threefold and sixfold symmetry). These multiunits buckling actuators made of buckling actuator units with different symmetries provide new patterns of parallel actuation. For example, the "nonbuckling centers" of the sixfold symmetry actuator are positioned in a triangular array instead of a square array in a fourfold symmetry case, and they rotate in the same directions instead of in a checkerboard pattern. One can also create patterns that consist of a mixture of buckling actuator units of different type, and create more variety in the patterns of collective motion.

Adv. Mater. **2015**,
DOI: 10.1002/adma.201503188

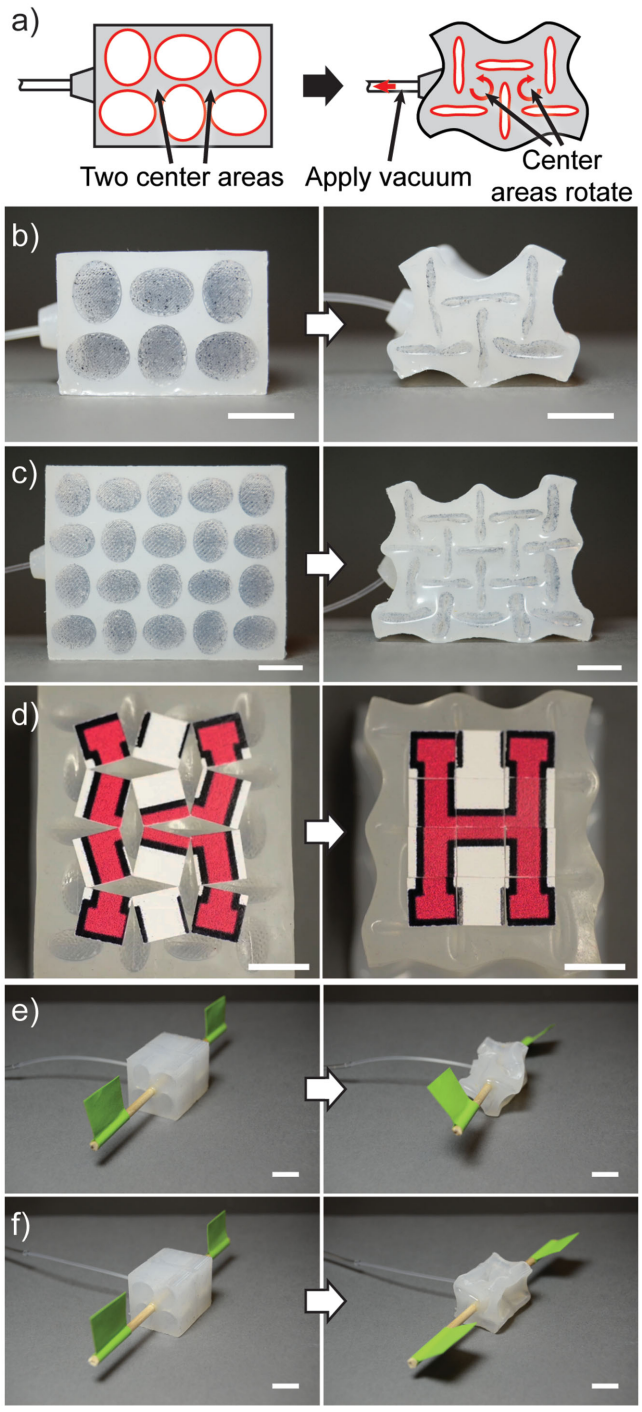

Figure 2. Parallel actuation and stackability of the buckling structure. a) Schematics of buckling actuator with two actuation units. b) Buckling actuator with two actuation units. c) Buckling actuator with 3 × 4 actuation units. d) Using buckling actuators to realize parallel actuation. The square tiles are simultaneously moved in a concordant way by the 3 × 4 buckling actuator to form the letter "H". e) Stacking two buckling actuators that rotate in the same direction. f) Stacking two buckling actuators that rotate in different directions. Scale bars are 1 cm.

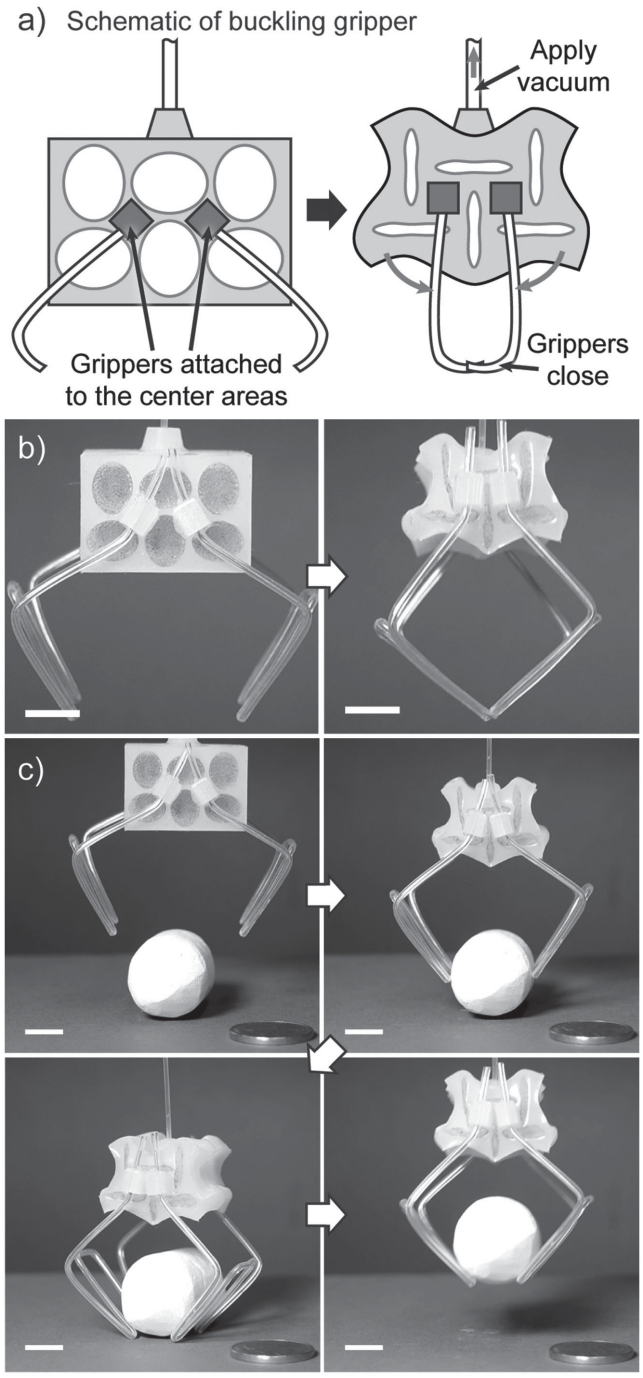

Figure 3. A soft gripper made of a buckling actuator. a) Schematics of the buckling gripper. b) The claws of the gripper close upon deflation of the buckling actuator. c) The buckling gripper picks up a piece of chalk. Scale bars are 1 cm.

The buckling actuator can be combined with both soft and hard components to perform useful functions. **Figure 3** shows a soft gripper, which we made by combining a two-unit buckling actuator with tubing-sheathed steel wires. This gripper closes its "claw" upon deflation, and reopens upon reinflation to atmospheric pressure (Figure 3a, Supporting video: gripper.mp4). Figure 3b shows that the buckling gripper can lift a piece of chalk (≈8.5 g, Supporting video: gripper_chalk.mp4). In frame 2, the gripper contacts the middle of the chalk; as it is lowered, it continues to close without additional control. This

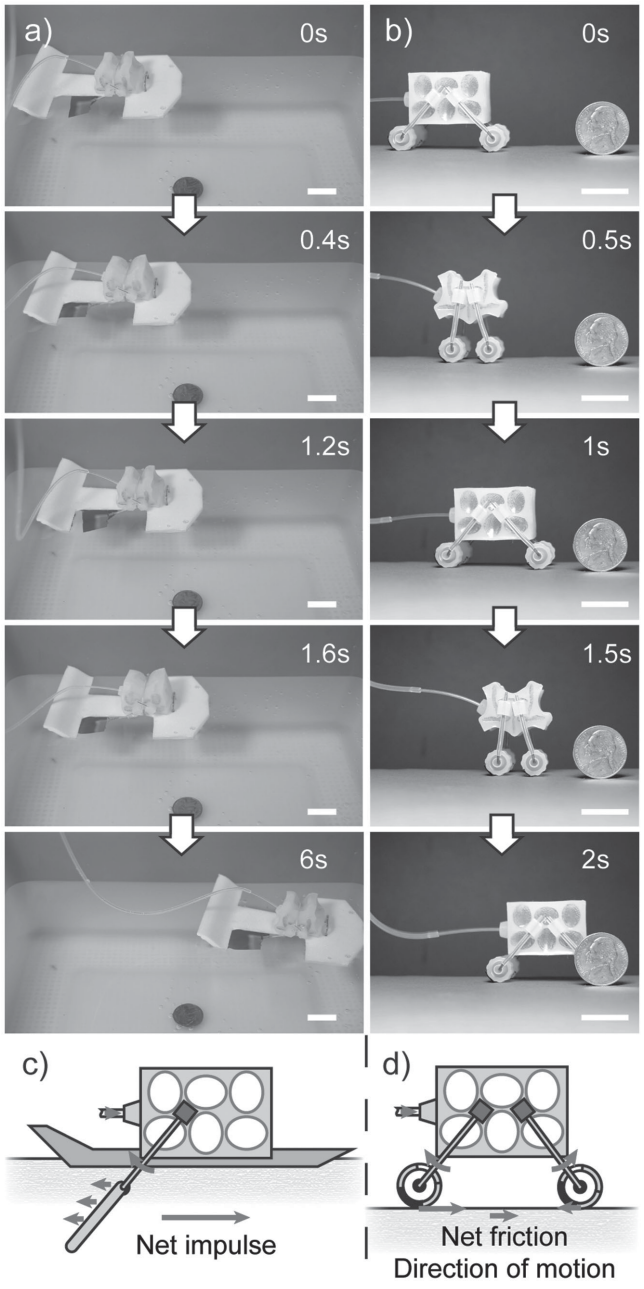

Figure 4. Soft robots with buckling actuators. a) A soft robotic swimmer. b) A soft robotic walker. c) Schematics of the swimmer. d) Schematics of the walker. Scale bars are 2 cm. The Supporting Information illustrates the motions of the swimmer and the cart in greater details.

type of adaptability is characteristic of many soft pneumatic-based systems.[5,9,10] This gripper can hold and lift objects of complex shapes (for example, a toy elephant; Figure S5a, Supporting Information, for Supporting video: gripper_toy.mp4), and a 50 g standard weight (Figure S5b, Supporting Information, for Supporting video: gripper_weight.mp4).

Soft buckling actuators have potential applications in devices that translate/locomote: they are light, and (in principle) adaptive to their environment. **Figure 4** shows two different types of soft robots designed to realize directed motion, both built with buckling actuators (Supporting videos: duck.mp4, cart.mp4). The first-a swimmer (loosely modeled as a duck)-moves forward due to an asymmetric design in the "feet," which can extend during the power stroke (i.e., inflation of the actuator), and fold during the return stroke. The "walker" is a four-wheeled "cart" whose legs move synchronously during a single cycle of evacuation and pressurization-two forward, two backward. It utilizes asymmetric friction in the feet: their rough sides in contact with the ground when the legs stride backward, and their smooth sides are in contact when the legs move forward. This asymmetry causes a unidirectional ratcheting movement (Figure S6, Supporting Information, for detailed schematics).

We further demonstrated an untethered version of the cart, which carries its own power supply, pump, valve, and circuit board (Figure S7 and S8, Supporting video: Autonomous Walker.mp4, details are in the Supporting Information). The system is thus capable of carrying the load required for autonomous operation (limited here to smooth flat surfaces). It is unoptimized, but demonstrates the potential for autonomous operation.

This paper describes a new strategy for actuating soft machines. It is based on a cooperative, reversible, buckling motion in structures consisting of a slab of an elastic polymer (or other elastic material) containing arrays of interacting beams and void spaces, when subjected to uniform compression. Previous studies of soft machines (grippers and tentacles)[5,9,10] have focused on actuations that produce motions based primarily on bending: e.g., grasping and walking. The buckling motions produced in the systems described here result in torsional motions, with angular rotations of ≈30°, localized at specific points in the structures.

These systems rely on negative pressure (vacuum), rather than positive pressure, for actuation. The use of negative pressure has both advantages and disadvantages. There are five major advantages: i) Shrinking on Actuation: Upon actuation (that is, on applying negative pressure by evacuating the void spaces in the structure), the device shrinks rather than expands (as it would in a soft machine actuated by positive pressure).[5,9,10,26] The shrinkage makes it possible to explore applications where an increase in volume would preclude this type of system (for example, in confined spaces, or in applications involving contact with tissue). ii) Torsional Motion: The motions produced from the buckling in these systems by applying negative pressure demonstrates new and more complex behaviors (i.e., cooperative buckling) than those (often simpler) stretching motions of soft machines actuated by positive pressure. iii) Safety: These systems are intrinsically safer for use around humans than those requiring highly compressed gases or liquids for actuation. There is little or no danger of rupture or explosion, or from formation of "aneurisms" (local "bulges around weak spots) from over-pressurization in these vacuum-activated devices. They should, therefore, be particularly appropriate for "cooperative" use with humans. iv) Lifetime: Because the strain on the elastomeric material is limited in each cycle of actuation, the lifetime of the system should, in principle, be higher than that in inflated systems subjected to relatively high strains. We have demonstrated experimentally that single-unit buckling actuators fabricated in Elastosil show no significant change in performance after a million cycles of

Adv. Mater. **2015**,
DOI: 10.1002/adma.201503188

actuation (Figure S9, Supporting Information). v) Scaling to Large Arrays: Because the structures that provide torsion can be scaled to large arrays, a very simple actuation (evacuation or pressurization) can cause the torsional movement of a large number of localized points.

A disadvantage of these systems is that the maximum force they can generate is limited by the pressure differential over which they operate: that is, between 1 atm and a fraction of atmosphere. (High vacuum is not required for these devices: the pressure on the device, when actuated, scales roughly as ΔP, and the difference between 0.1 and 0.001 atm of residual pressure in the device will not be significant for most applications.) The range over which pressure can be changed in applications at ambient atmospheric pressure will limit some applications requiring high force or very rapid actuation; for other applications (for example, in hyperbaric environments, or in applications in the deep sea) the use of reduced pressure to achieve motion could be an advantage. These buckling actuators provide new opportunities for the design of soft actuators and machines.

Supporting Information

Supporting Information is available from the Wiley Online Library or from the author.

Acknowledgements

This work was funded by a subcontract from Northwestern University under DOE Award No. DE-SC0000989. B.M. acknowledges the Wyss Institute for Biologically Inspired Engineering for salary support. B.L. was supported by the Harvard University work-study program for undergraduates. F.K. was supported by the NSF funded REU program under Award No. DMR-0820484. A.A. was supported by a Swedish Research Council (VR) post-doctoral fellowship.

Received: July 2, 2015
Revised: July 22, 2015
Published online:

[1] S. Vogel, *Cats' Paws and Catapults: Mechanical Worlds of Nature and People*, WW Norton & Company, New York **2000**.
[2] C. C. De Wit, G. Bastin, B. Siciliano, *Theory of Robot Control*, Springer-Verlag, New York **1996**.
[3] M. W. Spong, S. Hutchinson, M. Vidyasagar, *Robot Modeling and Control*, Vol. *3*, Wiley, New York **2006**.
[4] S. Kim, C. Laschi, B. Trimmer, *Trends Biotechnol.* **2013**, *31*, 287.
[5] F. Ilievski, A. D. Mazzeo, R. F. Shepherd, X. Chen, G. M. Whitesides, *Angew. Chem. Int. Ed.* **2011**, *123*, 1930.
[6] K. Suzumori, S. Iikura, H. Tanaka, *Proc. IEEE Int. Conf. MEMS*, IEEE, Piscataway, NJ, USA **1991**.
[7] K. Suzumori, S. Iikura, H. Tanaka, *Proc. IEEE Int. Conf. Rob. Autom.*, IEEE, Piscataway, NJ, USA **1991**.
[8] K. Suzumori, A. Koga, H. Riyoko, *Proc. IEEE Int. Conf. MEMS*, IEEE, Piscataway, NJ, USA **1994**.
[9] R. F. Shepherd, F. Ilievski, W. Choi, S. A. Morin, A. A. Stokes, A. D. Mazzeo, X. Chen, M. Wang, G. M. Whitesides, *Proc. Natl. Acad. Sci. USA* **2011**, *108*, 20400.
[10] R. V. Martinez, J. L. Branch, C. R. Fish, L. Jin, R. F. Shepherd, R. Nunes, Z. Suo, G. M. Whitesides, *Adv. Mater.* **2013**, *25*, 205.
[11] R. V. Martinez, C. R. Fish, X. Chen, G. M. Whitesides, *Adv. Funct. Mater.* **2012**, *22*, 1376.
[12] S. A. Morin, R. F. Shepherd, S. W. Kwok, A. A. Stokes, A. Nemiroski, G. M. Whitesides, *Science* **2012**, *337*, 828.
[13] B. Mosadegh, P. Polygerinos, C. Keplinger, S. Wennstedt, R. F. Shepherd, U. Gupta, J. Shim, K. Bertoldi, C. J. Walsh, G. M. Whitesides, *Adv. Funct. Mater.* **2014**, *24*, 2163.
[14] D. P. Holland, E. J. Park, P. Polygerinos, G. J. Bennett, C. J. Walsh, *Soft Robotics* **2014**, *1*, 224.
[15] C. Keplinger, M. Kaltenbrunner, N. Arnold, S. Bauer, *Proc. Natl. Acad. Sci. USA* **2010**, *107*, 4505.
[16] C. Keplinger, T. Li, R. Baumgartner, Z. Suo, S. Bauer, *Soft Matter* **2012**, *8*, 285.
[17] J.-S. Plante, S. Dubowsky, *Int. J. Solids Struct.* **2006**, *43*, 7727.
[18] X. Zhao, W. Hong, Z. Suo, *Phys. Rev. B* **2007**, *76*, 134113.
[19] X. Zhao, Z. Suo, *Appl. Phys. Lett.* **2007**, *91*, 061921.
[20] C. Wright, A. Johnson, A. Peck, Z. McCord, A. Naaktgeboren, P. Gianfortoni, M. Gonzalez-Rivero, R. Hatton, H. Choset, *Proc. IEEE Int. Conf. IROS*, IEEE, Piscataway, NJ, USA **2007**.
[21] T. Mullin, S. Deschanel, K. Bertoldi, M. Boyce, *Phys. Rev. Lett.* **2007**, *99*, 084301.
[22] K. Bertoldi, M. Boyce, S. Deschanel, S. Prange, T. Mullin, *J. Mech. Phys. Solids* **2008**, *56*, 2642.
[23] R. Bruzek, L. Biess, L. Al-Nazer, *Proc. ASME Jt. Rail Conf.* ASME, New York **2013**.
[24] J. Gordo, C. Guedes Soares, D. Faulkner, *J. Ship Res.* **1996**, *40*, 60.
[25] S. Timoshenko, J. M. Gere, *Theory of Elasticity Stability*, McGraw-Hill, New York **1961**.
[26] G. K. Klute, J. M. Czerniecki, B. Hannaford, *Proc. IEEE Int. Conf. Adv. Intell. Mechatron.*, IEEE, Piscataway, NJ, USA **1999**.

ADVANCED MATERIALS

Supporting Information

for *Adv. Mater.,* DOI: 10.1002/adma.201503188

Buckling of Elastomeric Beams Enables Actuation of Soft Machines

*Dian Yang, Bobak Mosadegh, Alar Ainla, Benjamin Lee, Fatemeh Khashai, Zhigang Suo, Katia Bertoldi, and George M. Whitesides**

Supporting Information

Buckling of Elastomeric Beams Enables Actuation of Soft Machines

*Dian Yang, Bobak Mosadegh, Alar Ainla, Benjamin Lee, Fatemeh Khashai, Zhigang Suo, Katia Bertoldi, and George M. Whitesides**

Fabrication of buckling actuators

We designed the molds using computer-aided design (CAD) (Solidworks) and fabricated them using a 3D printer (StrataSys Fortus 400mc). The molds, made of acrylonitrile butadiene styrene (ABS) plastic, were filled with a silicone-based elastomer (Ecoflex 0030) for at least 3 hours at room temperature (Figure S1). The buckling actuator is cast in two half structures and bonded together using uncured Ecoflex 00-30 in a 60 °C oven for 10 minutes. To interface with the actuator, we bonded a conically shaped elastomeric piece to the side of the buckling actuator to provide additional material for a tubing/air-duct to be attached (the extra conical piece prevents undesired leaking of air).

Measurement of angle of rotation vs. applied negative pressure

We measured the angles of rotations of the "non-buckling center areas" using a camera (Nikon D5100) and standard image analyzing software (FIJI). We added fiducial markers on the center areas using a marker pen before the measurement. We then took pictures and videos of the actuation process. The pictures and videos were then processed by FIJI to extract the angles of the marked lines. The values of the angles were subtracted by the initial value to produce the final angles of rotation at different pressures.

The pneumatic pressure was applied by a syringe, which was connected to a syringe pump (PHD 2000). The pressure values were measured by a pressure sensor (Honeywell ASDX005D44R) that was connected to the pressure transfer line, and read out using Labview.

Measurement of lifetime

We measured the lifetime of three single-unit buckling actuators fabricated in Elastosil by connecting them to an Arduino controlled/gated pneumatic source. The buckling actuators were each fully deflated and then re-inflated to the initial state repeatedly.

The buckling actuators were actuated at a frequency of 2Hz, and left running continuously for 5 days 19 hours, which resulted in more than 1000000 cycles of actuation. We tested the rotation angle vs. applied negative pressure of these three actuators, and no significant change in the curves was observed (Figure S9).

Choosing geometric parameters in designing the buckling actuators

A number of geometric parameters can be changed in designing the rotary buckling actuators (as illustrated in Figure 1, Figure S3) in order to change their mechanical properties. Important parameters include: the number of "buckling pillars," the width of these pillars, and the distance between the long axes of these pillars and the rotational center.

The number of "buckling pillars" affects the maximum angle the buckling actuator can achieve. As the number of pillars increase, the angle between two neighboring pillars (360° divided by the number of pillars) decreases. Figure S3 shows that the amplitude of rotation upon deflation decreases as the gap between the pillars become smaller. In order to reach a large angle of rotation, one ideally wants a small number of pillars (three, four, or five).

The widths of the pillars affect the pressure required for actuation as wider beams take higher pressure to compress. Since wider pillars require higher pressure to compress, they also provide more torque. The pillars need to be sufficiently wide to generate the required actuation vs. pressure curves, and to ensure that the structure is robust. It is also important to make the pillars sufficiently narrow that they buckle prior to the buckling of other unintended structural elements.

The distance between the long axes of these pillars and the rotational center also affects the torque the actuator can generate—a more off-centered pillar of the same width generates more torque (see equation S1, where F is the force applied, d is the distance between the force and the rotational center, and τ is the torque generated by the force). This higher torque comes at the cost of the maximum angle of rotation that can be achieved. Take the actuator in Figure 1 as an example: as one moves the pillars more off

center, the deflation chambers become more elongated, effectively reducing the amount of rotation needed to achieve full deflation.

$$\tau = F \times d \quad \text{(S1)}$$

In an industrial setting where one wants to optimize certain mechanical properties, finite element method (FEM) modeling can be used to optimize the performance of buckling actuators further. Simple geometric considerations can qualitatively predict many mechanical properties and aid the process of optimization.

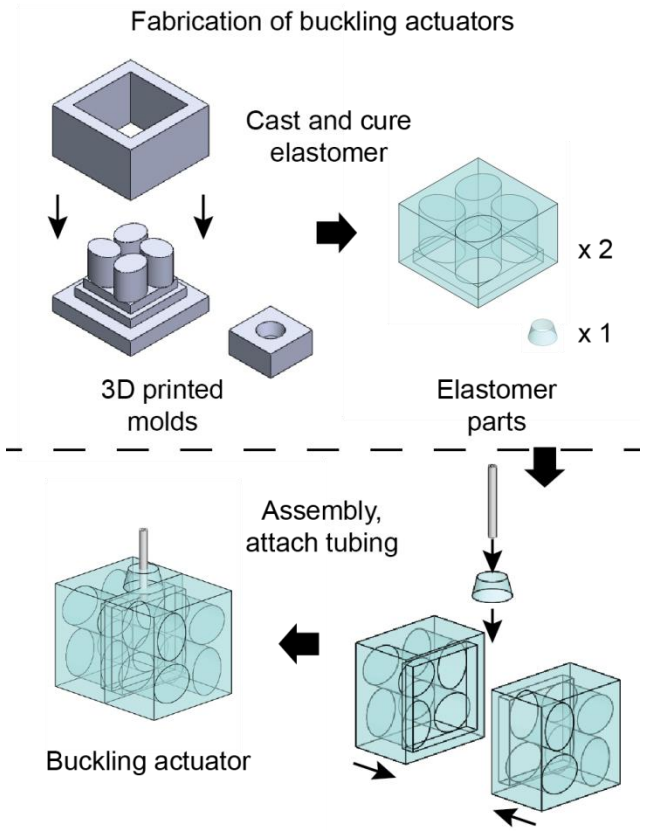

Figure S1. Fabrication of buckling actuator.

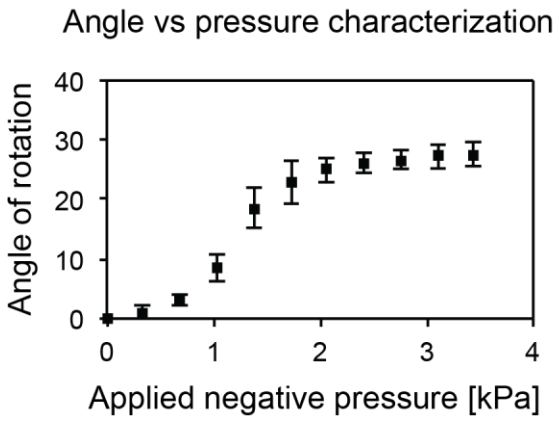

Figure S2 Angle of rotation vs. Applied negative pressure curves of a single-unit buckling actuator (1 atm = 100 kPa).

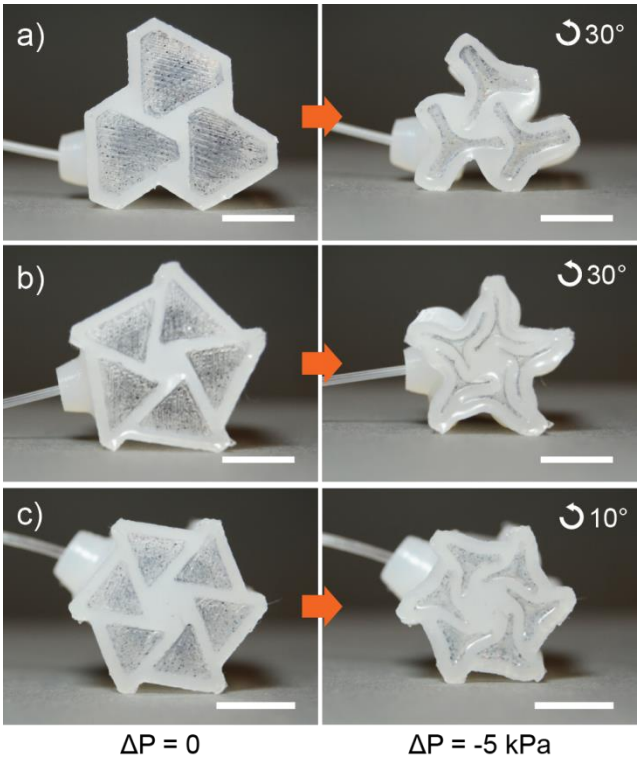

Figure S3. Examples of more buckling actuator geometries with different numbers of pillars. Scale bars are 1 cm.

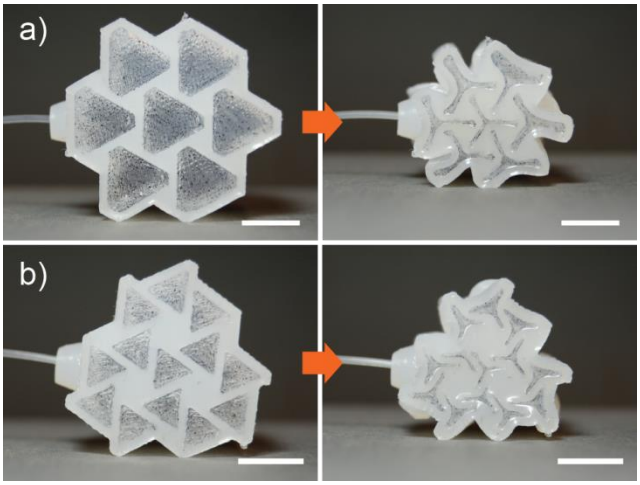

Figure S4. Parallel actuation in buckling actuator with different geometries. Scale bars are 1 cm.

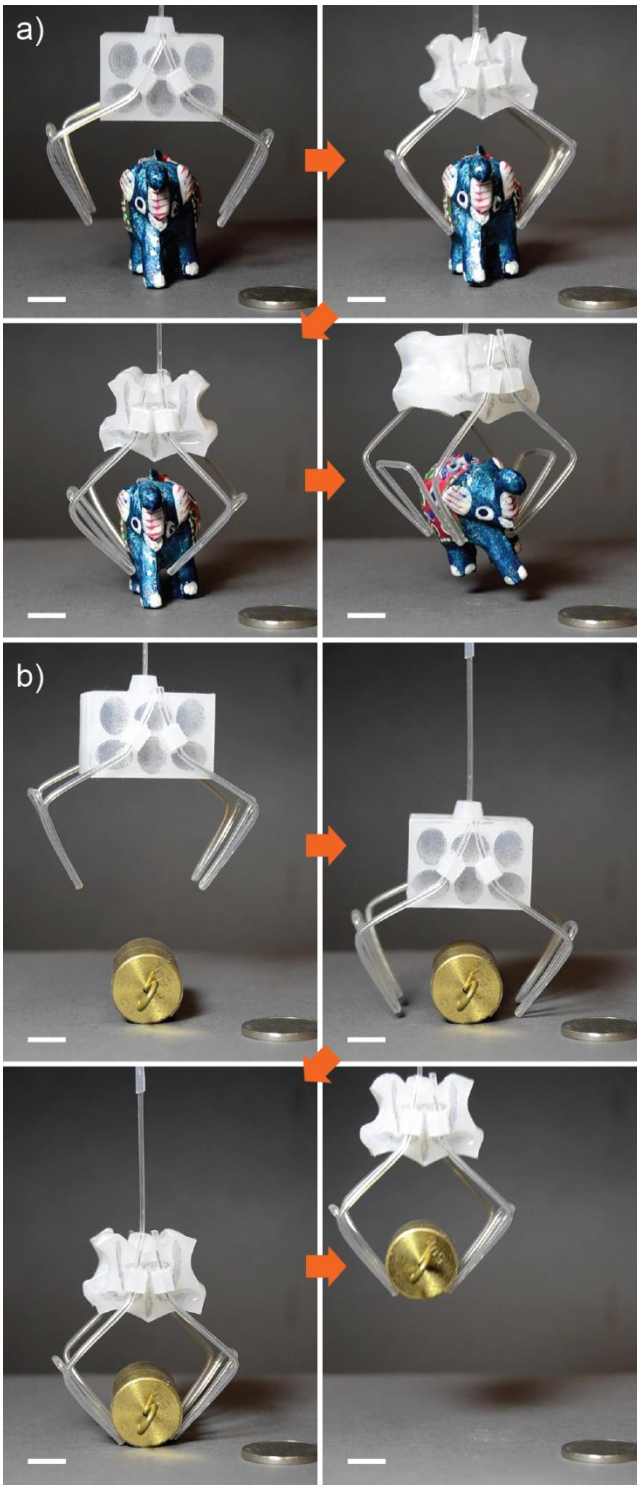

Figure S5. More examples of the buckling gripper. a) The buckling gripper picks up a toy elephant. b) The buckling gripper picks up a 50 g weight. Scale bars are 1 cm.

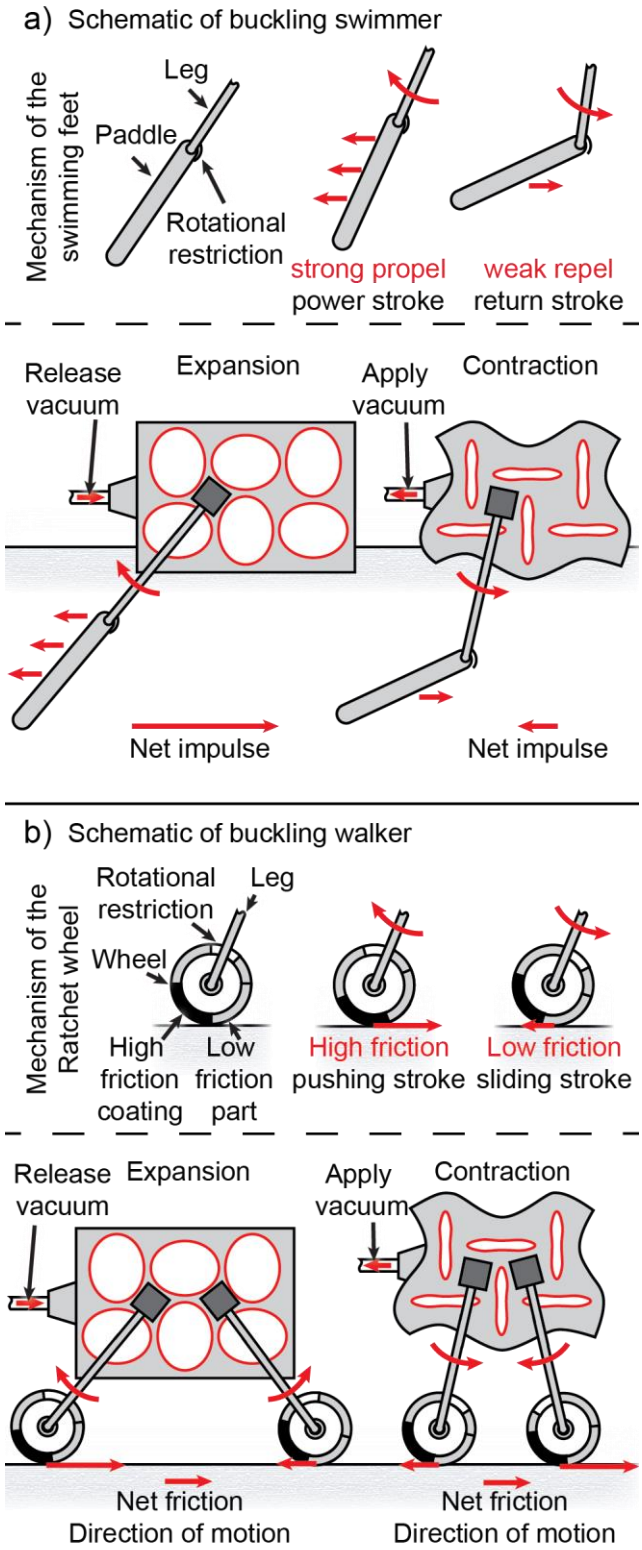
a) Schematic of buckling swimmer
Mechanism of the swimming feet
Leg
Paddle
Rotational restriction
strong propel
power stroke
weak repel
return stroke
Release vacuum
Expansion
Apply vacuum
Contraction
Net impulse
Net impulse
b) Schematic of buckling walker
Mechanism of the Ratchet wheel
Rotational restriction
Leg
Wheel
High friction coating
Low friction part
High friction
pushing stroke
Low friction
sliding stroke
Release vacuum
Expansion
Apply vacuum
Contraction
Net friction
Direction of motion
Net friction
Direction of motion

Figure S6. Detailed schematics of the buckling swimmer and the buckling walker.

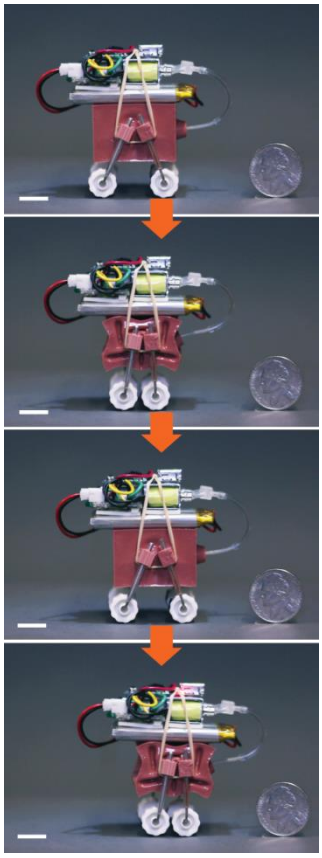

Figure S7. The soft robotic walker made untethered by carrying its own power supply, pump, valve, and circuit board. Scale bars are 1cm.

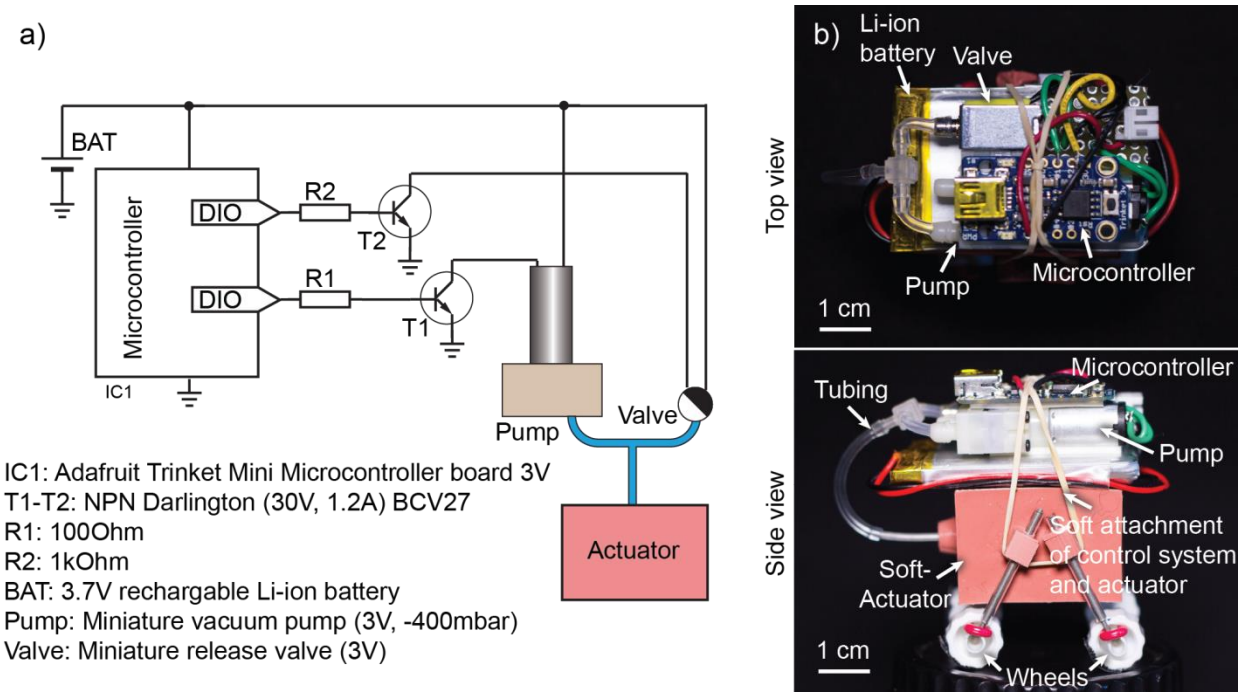

Figure S8. Circuit detail and schematics of the untethered soft robotic walker. Scale bars are 1 cm.

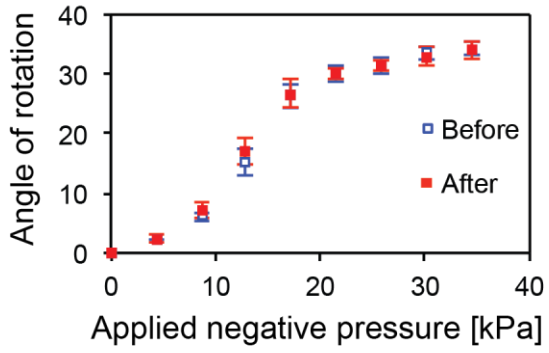

Figure S9 Comparison of the angle of rotation vs. applied negative pressure curve of three single-unit buckling actuator samples fabricated in Elastosil before and after 1000000 cycles of actuation at 2Hz.